

Cite this: *Anal. Methods*, 2025, **17**, 2302

# Rapid and accurate detection of huanglongbing in citrus by elasticity testing using a piezoelectric finger†

Pawan Rao,<sup>a</sup> Shu Huang,<sup>a</sup> Cheryl M. Armstrong,<sup>\*b</sup> Joseph Capobianco,<sup>b</sup> YongPing Duan,<sup>c</sup> Wei-Heng Shih<sup>ib</sup><sup>d</sup> and Wan Y. Shih<sup>ib</sup><sup>\*a</sup>

Rapid and sensitive detection of citrus huanglongbing (HLB) is critical for the control of this devastating disease. In this study, we have evaluated using a piezoelectric finger (PEF) with a 0.4 mm probe to measure the elastic modulus of a leaf to detect HLB in four different species of citrus including grapefruit (GFT), pumelo (PUM), lemon (LEM), and Valencia orange (VAL). Diseased citrus leaves were harvested from trees testing positive for the presence of *Candidatus Liberibacter asiaticus* (Las), the causal agent of HLB, and included both symptomatic leaves, which were blotchy mottle or yellowing and asymptomatic leaves, which did not display outward symptoms. Healthy leaves were harvested from trees testing negative for Las. The results indicated that the PEF elastic modulus test exhibited an overall 94% sensitivity and 90% specificity against the Las status of the trees for all four citrus types combined. Comparative quantitative real-time polymerase chain reaction (qPCR) tests on the same leaves showed an overall 89% sensitivity and 100% specificity against the Las status of the trees. While a Cohen–Kappa coefficient of 0.81 was obtained between the PEF and qPCR predictions, suggesting a “strong” agreement between the PEF and qPCR tests, a more detailed examination indicated that PEF was more sensitive overall in detecting the Las positive trees than qPCR, particularly from asymptomatic leaves for which PEF was 96% sensitive versus 78% sensitive by qPCR, indicating the potential of using PEF for early detection of HLB.

Received 24th October 2024  
Accepted 9th February 2025

DOI: 10.1039/d4ay01952k

rsc.li/methods

## 1. Introduction

While citrus is susceptible to multiple different pathogens, *Candidatus Liberibacter asiaticus* (Las) is currently the pathogen of greatest concern in the United States and elsewhere.<sup>1–5</sup> Las, an alpha-proteobacterium, has been associated with the disease known as huanglongbing (HLB or citrus greening). The disease has been found to affect all members of the genus *Citrus* and is systemic in the plant. Therefore, symptoms can be found on the leaves, fruit, and roots and include the presence of leaf mottling, yellow shoots, and the production of small lopsided fruit with a bitter taste and aborted seeds.<sup>6,7</sup> Twig/branch dieback, increased early fruit drop, and death of the tree are all markers of advanced disease states. The disease is primarily

spread by its insect vector, *Diaphorina citri* Kuwayama (Asian citrus psyllid, ACP), although transmission *via* grafting and dodder (*Cuscuta pentagona*) is also possible.<sup>7,8</sup>

Current control efforts in locations where HLB is already widespread include the use of insecticide programs to reduce the psyllid population and the application of additional nutrients/amendments to help extend the production life of HLB-affected citrus trees.<sup>9,10</sup> In locations where the presence of HLB is sparse, such as California, USA, roguing of infected trees is also being used to help prevent spread. Nevertheless, complete eradication in California has proven difficult over the years because of the possibility of multiple introductions of the disease to the area,<sup>11</sup> the consistent presence of the psyllid in the citrus-producing areas,<sup>12</sup> and the long latency period of the disease leading to difficulties in identifying infected trees.<sup>13</sup> Broad surveys are being conducted in citrus-producing regions of California entailing the testing of both psyllids and plants *via* quantitative polymerase chain reaction (qPCR) as a proactive measure for identifying the presence of Las in a timely fashion.<sup>14</sup> However, several issues associated with disease detection threaten the effectiveness of these surveys such as the uneven distribution of the pathogen in the plant,<sup>15</sup> the reliance upon a lab-based testing method for detection, the presence of low titers of pathogen, and the fact that plants are typically

<sup>a</sup>School of Biomedical Engineering, Science, and Health Systems, Drexel University, Philadelphia, PA 19104, USA. E-mail: shihw@drexel.edu

<sup>b</sup>Eastern Regional Research Center, USDA, Agricultural Research Service, 600 East Mermaid Lane, Wyndmoor, PA, 19038, USA. E-mail: cheryl.armstrong@usda.gov

<sup>c</sup>U. S. Horticultural Research Laboratory, 2001 South Rock Road, Fort Pierce, FL 34945, USA

<sup>d</sup>Department of Materials Science and Engineering, Drexel University, Philadelphia, PA 19104, USA

† Electronic supplementary information (ESI) available. See DOI: <https://doi.org/10.1039/d4ay01952k>



asymptomatic especially during the early stages of infection. Therefore, new methods that increase detection efficiency and are applicable to field-based testing are urgently needed.

Attempts at the development of visual sensors to detect starch accumulation have been made. However, the sensors often suffer from an inability to distinguish zinc-deficiency from HLB-triggered blotchy mottle without further processing (such as grinding) of the leaves.<sup>16</sup> Visual methods also do not address early detection prior to symptom development since asymptomatic leaves are not distinguishable from healthy leaves. Canine olfactory detection has also been explored for in-field detection.<sup>17</sup> However, canines are expensive due to their need for training and their sensitivity can vary wildly from dog to dog.<sup>17</sup> There is an immediate need for an HLB detection tool that is rapid, accurate, field-usable, and inexpensive that citrus growers can employ as an in-field screening tool to identify Las-infected plants early for further qPCR diagnosis to prevent the spread of HLB disease.

Changes to the leaf tissue at an anatomical level that correlate with infection by Las have been noted in citrus. These include middle lamella swelling/phloem necrosis, obstruction of sieve elements resulting from the deposition of callose and phloem protein,<sup>7,18</sup> and the disruption of chloroplast structure caused by starch accumulation.<sup>19–22</sup> Although these changes appear to occur universally across the different citrus species upon infection and may act as a good indicator for the presence of Las, discovery of these changes was made by microscopy. Since microscopy is not a technique that is easily adaptable to rapid detection in the field, alternative approaches for identifying such changes may be more applicable to disease detection. Anecdotal observation suggests these Las-caused anatomical changes not only are visible under a microscope but also manifested in leaf stiffness palpable by an experienced researcher. Given this information, tissue elasticity may be a means to quantitatively measure the changes that are occurring at the cellular level in Las-infected citrus leaves as there is precedence for this in other systems.

For example, a piezoelectric finger (PEF), as schematically shown in Fig. 1(a), is a piezoelectric cantilever *in situ* tissue elasticity sensor that has been shown to serve as a device for detecting breast cancers.<sup>23,24</sup> The ability to apply this method to breast cancer relies on cellular alterations that are occurring, making the cancerous tissues harder than the surrounding tissues.<sup>23–29</sup> The PEF works by applying an external voltage to the driving piezoelectric layer, which bends the cantilever, and thereby generates a force at the cantilever tip *via* the “converse piezoelectric” effect. When the cantilever is bent, the sensing piezoelectric layer at the bottom generates an induced voltage that can be used to quantify the displacement at the cantilever tip *via* the “direct piezoelectric” effect. Using this principle, a handheld breast cancer detector consisting of an array of four PEFs has demonstrated the capability of quantifying breast tissue elasticity non-destructively and *in vivo*.<sup>23,24</sup> By contrasting the higher elastic moduli of the cancerous tissues with those of the surrounding healthy tissues,<sup>24</sup> a sensitive detector for breast cancers was created. This handheld, field-portable breast cancer detector was commercialized under the iBreastExam (iBE) and is currently in use in several developing countries (iBreastExam.com).

Because leaves from HLB-affected trees appear harder than healthy leaves, we systematically investigated leaf elasticity using a PEF to detect HLB in citrus, and therefore first demonstrated the correlation between leaf elasticity and Las infection and provided a new tool for rapid and sensitive detection of HLB.

## II. Materials and methods

### II.1. Citrus leaves

Both healthy and HLB-affected plants were maintained in an insect-proof greenhouse located at the US Horticultural Research Laboratory (USHRL) in Fort Pierce, FL. They encompassed the four major citrus species/hybrids: (1) *Citrus × paradisi* noted as Grapefruit (GFT), (2) *Citrus × sinensis* noted as Valencia (VAL), (3) *Citrus × limon* noted as Lemon (LEM) and (4) *C. maxima* noted as Pummelo (PUM). The HLB-affected plants utilized were obtained by grafting HLB-affected scions from *Citrus × limon* onto the other citrus plants listed above. To confirm the presence of HLB post graft inoculation and determine the overall Las status of the tree, symptomatic leaves from HLB-affected citrus plants were tested for the presence of Las using qPCR with Las-specific primers.<sup>15</sup> In this study, leaf samples that displayed typical HLB symptoms and those that appeared asymptomatic were collected from the qPCR confirmed trees, which ranged from two to six years old. Healthy plants were not infected with Las and tested negative for its presence.

Branches of each type of plants were harvested, placed in a clearly-labeled 12"×12" zip-lock bag. All the bags were then placed in a Styrofoam box packed with ice bags to keep cool and shipped overnight to Shih's lab in Philadelphia, PA. Upon receipt of the package, these branches were stored at 4 °C in their original zip-lock bags with damp paper towels in the bags to minimize drying. Mature leaves 6–10 cm long of each type

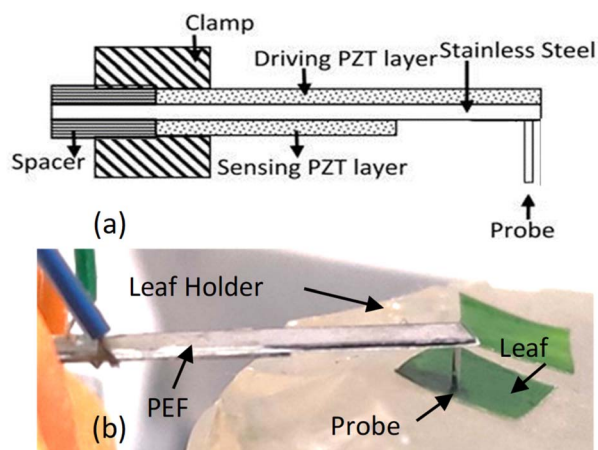


Fig. 1 (a) A schematic of a piezoelectric finger (PEF) and (b) a photograph of a PEF during leaf testing with its probe on the leaf segment, which lies upon a soft leaf sample holder.



were selected from different branches in each bag. Small areas of about 5 mm × 5 mm of a leaf close to the stem that were flat without coarse veins were selected for testing. The leaf sample were laid on the leaf sample holder with the underside (abaxial) up and pressed firmly against the gelatin leaf sample holder with the back of the bent-tipped tweezers such that no air pockets existed between the leaf sample and the surface of the leaf holder to ensure the elasticity measurements were accurate (Fig. S1 in ESI†). Furthermore, to examine whether the elasticity of symptomatic leaves differ from that of asymptomatic leaves, samples of symptomatic leaf were taken from areas of the leaves that looked visibly diseased (yellowed or mottled) in addition to being close to the stem. Sample thickness was measured with a caliper (Fisher) at three different locations.

Grapefruit samples were divided into four subgroups: healthy/Las<sup>-</sup> (GFT-1G), asymptomatic/Las<sup>+</sup> (GFT-2G), blotchy mottle/Las<sup>+</sup> (GFT-3G), and yellow/Las<sup>+</sup> (GFT-4G). Valencia samples were divided into four subgroups: healthy/Las<sup>-</sup> (VAL-1G), asymptomatic/Las<sup>+</sup> (VAL-2G), symptomatic/Las<sup>+</sup> (VAL-3G), and yellow/Las<sup>+</sup> (VAL-4G). Lemon samples were divided into three subgroups: healthy/Las<sup>-</sup> (LEM-1G), asymptomatic/Las<sup>+</sup> (LEM-2G), and symptomatic/Las<sup>+</sup> (LEM-3G). Pummelo samples were divided into three subgroups: healthy/Las<sup>-</sup> (PUM-1G), asymptomatic/Las<sup>+</sup> (PUM-2G), and symptomatic/Las<sup>+</sup> (PUM-3G). In this study, “healthy/Las<sup>-</sup>” leaves were harvested from trees testing negative for Las while both “asymptomatic/Las<sup>+</sup>” and “symptomatic/Las<sup>+</sup>” leaves were harvested from trees testing positive for Las. Leaves classified as symptomatic displayed typical symptoms of HLB such as blotchy mottle or yellowing and those classified as asymptomatic did not display any outward symptoms of HLB. It is worth noting that asymptomatic and healthy leaves are indistinguishable upon visual inspection, even to a trained plant pathologist, despite the presence of Las in asymptomatic leaves. Six leaves ranging from young (small) to mature (long) were tested for each group. Leaf length and width were measured using a ruler and photographs were taken to document leaf characteristics (Fig. S2 in ESI†). The reason we had only six leaves in each group (except healthy GFT) was because for this study we could only conduct manual tests using lab equipment, which was slow. In the meantime, there were 16 distinct groups to test in only two days to avoid potential leaf drying or rotting, which could affect the measured elastic modulus values. Having three distinct types of Las<sup>+</sup> leaves for each citrus species allowed the measured elastic moduli values of any two types to be compared reliably. Therefore, even though there were only six leaves in each group, the inclusion of three different Las<sup>+</sup> groups for each citrus species effectively increased the number of Las<sup>+</sup> leaves of each species to 18 while permitting the comparison among distinct groups. This helped to overcome the shortcoming of six leaves per group and enhanced the reliability of the statistics.

## II.2. PEF leaf elasticity tester

The PEF used was 22 mm long and 4 mm wide. Both the driving and sensing piezoelectric layers were 127 μm thick lead zirconate titanate (PZT) (5H, T105-H4NO-2929, Piezo.com) with the

driving PZT being 22 mm long and 4 mm wide while the sensing PZT was 12 mm and 4 mm wide. The middle support layer was 50 μm thick stainless-steel (Alfa Aesar) that was 22 mm long and 4 mm wide. For leaf testing, a 4 mm long brass rod (Albion Alloys) with a 0.4 mm diameter was attached to the stainless-steel side (underside) of the free end of the cantilever using a nonconductive epoxy to serve as the “probe” of the PEF (Fig. 1(a) and (b)). A direct current (DC) voltage was applied using a function generator (Agilent 33220A) at 0.1 Hz. The entire assembly was then affixed to a XYZ positioner (OptoSigma) using a c-clamp (Pony Jorgensen, USA).

## II.3. Thin probe and soft leaf sample holder

Although the premise behind the use of the PEF for measuring leaves is consistent with that of the previously described use of the PEF to measure breast tissue,<sup>23–29</sup> modifications to the device and the setup were needed to ensure meaningful leaf elastic modulus measurements capable of differentiating Las infected and non-infected leaves. One modification was the use of a very thin probe to contact the leaf sample as illustrated in Fig. 1(b). The depth sensitivity of the PEF elasticity sensor is known to be twice the diameter of the probe contacting the material being tested.<sup>27,28</sup> While a very thin probe is more likely to produce an elastic modulus close to that of the leaf, it is also more likely to poke into the leaf and produce erroneous elastic modulus measurements. To avoid such pitfalls, probes with a diameter larger than the leaf thickness were used where a PEF measurement assesses not only the elasticity of the leaf but also part of the leaf sample holder under the leaf. To prevent the measured elastic moduli from being overwhelmed by a hard sample holder, a gelatinous leaf sample holder that was softer than the leaf samples was utilized. The sample holder consisted of a gelatin gel stored in a Petri dish sealed with paraffin. When in use, the gelatin gel was flipped over so that the bottom side was in contact with the leaf samples. Care was also taken to ensure that the leaf sample was in complete contact with the gel sample holder and there was no air pocket between the leaf sample and the gel sample holder to inadvertently affect the value of the measured elastic modulus.

Elastic modulus measurements obtained using the PEF described above with its gelatin leaf holder were compared to those taken using the Instron machines (MTS Criterion Model 43 and BOSE ElectroForce 3200 Series II Test Instruments) to verify the elastic modulus measurement performance. In addition, prior to each leaf sample testing session, the elastic modulus of the gelatin leaf holder was tested to confirm that the PEF was working properly. The elastic modulus of a leaf was measured by simply placing the probe of the PEF on top of the leaf and applying a DC voltage, 2, 3, 4, 5, 6, and 7 V approximated by a 0.1 Hz square wave function provided by an Agilent 33220A voltage supply to the driving PZT layer to exert a force on the leaf, which induced a corresponding piezoelectric voltage across the sensing PZT layer and was measured by an oscilloscope (Agilent Technologies DSO3062A). These induced voltages,  $V_{in}$  together with the induced voltage without a sample,  $V_{in,0}$  (see Fig. 2(a)) were then arranged in a plot of



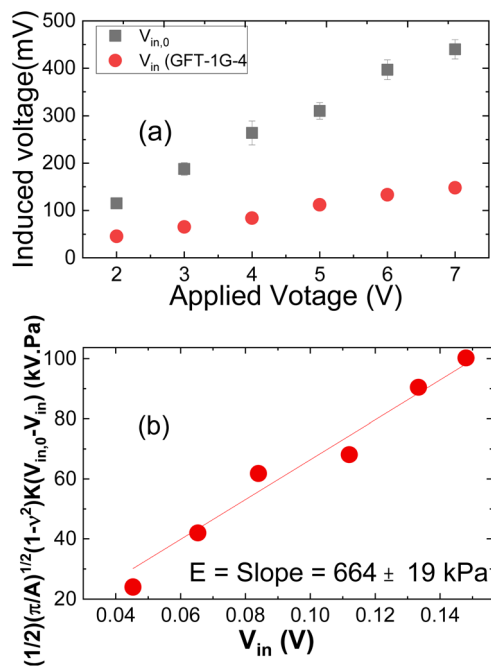


Fig. 2 (a)  $V_{in,0}$  and  $V_{in}$  versus applied voltage, and (b)  $(1/2)(\pi/A)^{1/2}(1 - \nu^2)K(V_{in,0} - V_{in})$  versus  $V_{in}$ . The slope in (b) yields the elastic modulus,  $E$ .

$(1/2)(\pi/A)^{1/2}(1 - \nu^2)K(V_{in,0} - V_{in})$  versus  $V_{in}$  as shown in Fig. 2(b) where  $\nu = 0.5$  is Poisson's ratio of the leaf sample,  $A$  is the contact area of the probe, and  $K = 158 \text{ N m}^{-1}$  is the effective spring constant of the PEF determined from a force versus displacement curve generated with weights and a Keyence laser displacement meter (Keyence) measurements as previously described.<sup>25,26</sup> The slope  $E$ , of the leaf sample was then deduced as slope of the regression of the least squared fit of this plot and the standard deviation the root mean squared error to the regression as shown in Fig. 2(b).<sup>23–29</sup> The elastic modulus values of each leaf sample were measured three times ( $n = 3$ ).

#### II.4. Determining the presence/absence of Las via qPCR

Although trees from which we harvested the leaves had a known Las status, it is unclear if every leaf from the same tree would have the same amount of Las or elastic modulus. For this reason, we performed qPCR on each leaf tested by PEF for comparison. Total genomic DNA was extracted from all leaves examined by the PEF using a modified Qiagen DNeasy Plant mini kit protocol (Qiagen, Germantown, MD) as described previously<sup>30</sup> using the midrib of each of the leaves. Assessment of the extracted DNA was performed using the DeNOVIX DS-11+ spectrophotometer (DeNOVIX, Wilmington, DE). DNA was stored at  $-80^\circ\text{C}$  until assayed for the presence/absence of Las. Assays for the presence/absence of Las were performed using the Applied Biosystems StepOnePlus Real-Time PCR System (ThermoFisher Scientific, Waltham, MA) using the Las specific 16S rDNA primer/probe set.<sup>31</sup> TaqMan Fast Universal PCR Master Mix ( $2\times$ ), No AmpErase UNG (Life Technologies, Foster City, CA) was used in conjunction with the HLBasf/HLBr (5 nmol) primers and HLBp (2.5 nmol) probe, and  $\sim 100$  ng of total

genomic DNA in a reaction volume totalling 15  $\mu\text{L}$ . Amplification was performed in triplicate using the 'fast' temperature mode using cycling parameters previously described.<sup>30</sup> The presence of Las was defined as threshold cycle (Ct) values  $< 36$  because a blind evaluation of the primer pair used in this study by 10 different laboratories in 4 different states indicated that the greatest sensitivity with minimal loss in specificity was achieved with a Ct of 36.<sup>32,33</sup> An internal control targeting the single-copy nuclear malate dehydrogenase (MDH) gene was used in conjunction with the HLBasf/HLBr primer and HLBp probe set above as previously described.<sup>14</sup>

#### II.5. Statistical analysis

The receiver operating characteristic (ROC) curves, sensitivities, and specificities of the PEF tests were determined against the Las status of the trees from which the leaves were harvested using MATLAB R2020b software with graphs being plotted in Origin 2017 (Origin Lab).

In addition, how well the predictions based off PEF elastic modulus measurements agree with the predictions based off qPCR results was analysed using Cohen-Kappa coefficient,  $K$ , defined as<sup>34</sup>

$$K = (p(a) - p(e))/(1 - p(e)), \quad (1)$$

with  $p(a)$  representing the fraction of tests that are in actual agreement between the PEF and qPCR predictions, defined as<sup>34</sup>

$$p(a) = (a + b)/n, \quad (2)$$

and  $p(e)$  representing the fraction of tests the agreement between PEF and qPCR predictions is by chance, defined as<sup>34</sup>

$$p(e) = [(a + d)(a + c)/n + (c + b)(d + b)/n]/n, \quad (3)$$

where  $a$  is the number of tests for which both PEF and qPCR predictions are positive,  $b$  is the number of tests for which both PEF and qPCR predictions are negative,  $c$  is the number of tests for which qPCR prediction is negative but PEF prediction is positive and  $d$  is the number of tests for which qPCR prediction is positive but the PEF prediction is negative, and  $n = a + b + c + d$  is the total number of tests.

## III. Results

### III.1. Effect of probe diameter

To examine how the probe diameter affected the sensitivity of a PEF to differentiate healthy and Las<sup>+</sup> using the setup as shown in Fig. 1(b), we plotted  $V_{in,0} - V_{in}$  of the healthy (squares) and Las<sup>+</sup> (circles) leaves measured with a PEF with a 0.6 mm probe and a PEF with a 0.4 mm probe in Fig. 3(a) and (b), respectively. We also plotted leaf thickness (Fig. 3(c) and (d)) for comparison with  $V_{in,0} - V_{in}$  measurements. Results indicate the  $V_{in,0} - V_{in}$  measurements using a PEF with either a 0.6 mm probe or a 0.4 mm probe could more reliably differentiate the Las<sup>+</sup> leaves from Las<sup>-</sup> leaves than the leaf thickness. However, when using a PEF containing a 0.6 mm probe, overlap is seen amongst the



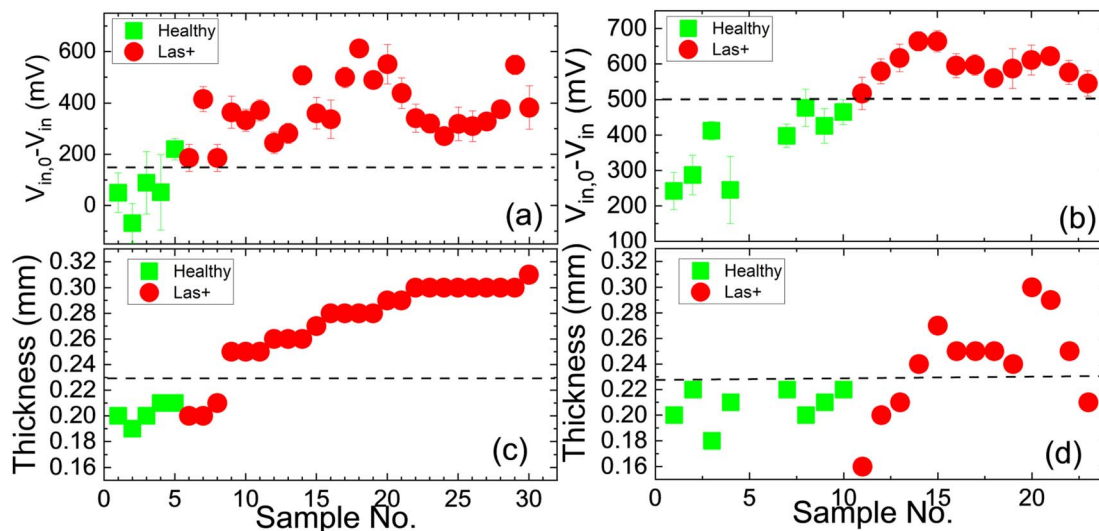


**Fig. 3**  $V_{in,0} - V_{in}$  (top graphs (a) and (b)) and thickness (bottom graphs (c) and (d)) of leaves containing the bacterium (circles = Las<sup>+</sup>) as compared to those without (squares = Las<sup>-</sup>) when using a probe with a diameter of either 0.6 mm (a and c) or 0.4 mm (b and d).  $V_{in,0} - V_{in}$  of a single leaf sample were taken three times and the average of those measurements shown. Error bars represent standard deviation of the mean. Absent error bars indicate error bars are smaller than the symbol size.

$V_{in,0} - V_{in}$  measurements of leaves containing the bacterium (Las<sup>+</sup>) as compared to those without (Las<sup>-</sup>). This overlap is not evident in the  $V_{in,0} - V_{in}$  measurements using a 0.4 mm probe, indicating the 0.4 mm probe is more sensitive to the elastic modulus differences resulting from the diseased state of the leaves. Based upon this empirical evidence, a probe diameter of 0.4 mm was utilized throughout the remainder of the study.

### III.2. Las detection by elastic modulus measurements of GFT, PUM, LEM, and VAL

As an example, the elastic moduli of all the subtypes of GFT as measured by the PEF with a 0.4 mm probe are shown in Fig. 4(a) and receiver operating characteristic (ROC) curve of diseased GFT leaves vs. healthy leaves is shown in Fig. 4(b). The

horizontal dashed line in Fig. 4(a) indicates the cutoff elastic modulus value deduced from the elastic modulus distribution of the Las<sup>+</sup> and Las<sup>-</sup> leaves shown in the inset (I) of Fig. 4(b) that were used to determine the presence of Las. In general, the elastic moduli of Las<sup>+</sup> subgroups, including the asymptomatic subgroup, were mostly above those of the healthy (Las<sup>-</sup>) subgroups and above the dashed line. This is also reflected in the bimodal distribution seen for the elastic moduli, with the Las<sup>+</sup> subgroup demonstrating good separation from the Las<sup>-</sup> subgroup (see inset (I) of Fig. 4(b)) for all four Las<sup>+</sup> groups and resulting in the square-looking receiver operating characteristic (ROC) curves for all groups as shown in Fig. 4(b). The sensitivity and specificity of each group were determined using the cutoff elastic modulus as indicated by the vertical dashed line where

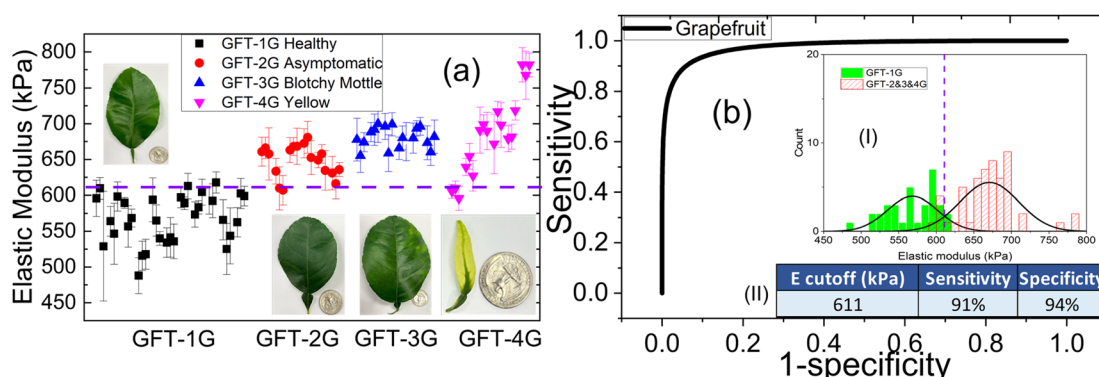


**Fig. 4** Detection of HLB in GFT at early and late stages of infection using the PEF. (a) Elastic modulus comparison amongst GFT leaves: Healthy GFT-1G (Las<sup>-</sup>), Asymptomatic GFT-2G (Las<sup>+</sup>), Blotchy mottle GFT-3G (Las<sup>+</sup>) and Yellow GFT-4G (Las<sup>+</sup>) where the dashed line represents the cutoff value selected for differentiation of Las<sup>+</sup> from Las<sup>-</sup> samples, and (b) receiver operating characteristic (ROC) curve for healthy (GFT-1G) vs. diseased GFT leaves derived from the distribution of elastic modulus values in between Las<sup>-</sup> (GFT-1G) and Las<sup>+</sup> (GFT-2G, GFT-3G and GFT-4G) GFT leaves shown in inset (I) of (b), insets (II) in (b) is a table showing the cutoff elastic modulus value deduced from distribution shown in insets (I) in (b), and the sensitivity and specificity between healthy and diseased GFT leaves.



**Table 1** Sensitivity and specificity of PEF elastic modulus and those of qPCR for GFT, PUM, LEM, VAL and all leaves. Note for both PEF and qPCR, the sensitivity and specificity here were derived against the Las status of the trees. These results indicate that qPCR and PEF are both sensitive and specific in detecting HLB but PEF is more sensitive than qPCR (94% sensitivity of the former *versus* 89% of the latter) while qPCR is more specific than PEF (100% specificity of the former *versus* 90% of the latter)

	PEF		qPCR	
	Sensitivity	Specificity	Sensitivity	Specificity
GFT	91%	94%	78%	100%
PUM	97%	94%	83%	100%
LEM	89%	83%	97%	100%
VAL	98%	83%	100%	100%
All	94%	90%	89%	100%

the healthy/Las<sup>-</sup> and Diseased/Las<sup>+</sup> distributions crossed in the inset (I) of Fig. 4(b). The resultant sensitivity and specificity of the PEF testing respectively are 91% and 94% for GFT and shown in the table of inset (II) in Fig. 4(b). Clearly, in all four groups, the PEF's elastic modulus measurements were able to differentiate Las<sup>+</sup> from Las<sup>-</sup> leaves, including distinguishing asymptomatic leaves from healthy leaves, with a high degree of sensitivity and specificity. The complete elastic modulus comparison plots and ROC curves of all four citrus species/hybrids – GFT, PUM, LEM, and VAL are shown in Fig. S3 in ESI.† A summary of the sensitivities, and specificities of all four citrus species of leaves and the average sensitivity and specificity of all citrus leaves are given in Table 1. When combining all the citrus leaves from the 267 tests conducted, the PEF elastic modulus measurements achieved an overall 94% sensitivity and 90% specificity. Note that the sensitivities and specificities shown were based upon the Las status of the trees, as we assumed all leaves from the same tree had the same Las status. This means that PEF elastic modulus measurements could determine the Las status of a tree with an overall 94% sensitivity and 90% specificity, suggesting PEF elastic modulus testing on individual leaves could be a sensitive and specific tool for determining the presence of Las within a tree, even if the leaves display no visual symptoms, *i.e.*, asymptomatic.

### III.3. Comparisons with qPCR

Every leaf tested by the PEF was also tested by qPCR in triplicate. The cutoff cycle threshold, Ct, values by qPCR has been defined as 36 for all citrus species/hybrids.<sup>15</sup>

**III.3.1 Comparison through Cohen–Kappa coefficient.** The Cohen–Kapper coefficient was used to evaluate the consistency amongst the PEF predictions and qPCR predictions based upon the cutoffs stated above. In Table 2, we listed values for  $n$ ,  $a$ ,  $b$ ,  $c$ ,  $d$ , and  $k$  for GFT, PUM, LEM, and VAL leaves where  $a$  is the number of tests for which both PEF and qPCR are positive,  $b$  is the number of tests for which both PEF and qPCR are negative,  $c$  is the number of tests for which qPCR is negative but PEF is positive and  $d$  is the number of tests for which qPCR is positive but the PEF is negative, and  $n = a + b + c + d$  is the total number

**Table 2** Values for  $n$ ,  $a$ ,  $b$ ,  $c$ ,  $d$ , and  $k$  for GFT, PUM, LEM, and VAL leaves where  $a$  is the number of tests for which both PEF and qPCR are positive,  $b$  is the number of tests for which both PEF and qPCR are negative,  $c$  is the number of tests for which qPCR is negative but PEF is positive and  $d$  is the number of tests for which qPCR is positive but the PEF is negative, and  $n = a + b + c + d$  is the total number of tests, and  $k$  is the Cohen–Kappa coefficient calculated using eqn (1)–(3). As can be seen, the overall  $k$  is 0.81. A Cohen–Kappa coefficient of 0.81 or above is indicative of “strong” or “almost perfect agreement” between the two methods

Cohen–Kappa coefficient for PEF–qPCR comparison						
Citrus	$n$	$a$	$b$	$c$	$d$	$k$
GFT	87	49	31	5	2	0.83
PUM	54	36	14	0	4	0.82
LEM	54	32	15	4	3	0.71
VAL	72	53	15	1	3	0.84
All	267	170	75	10	12	0.81

of tests, and  $k$  is the Cohen–Kappa coefficient calculated using eqn (1)–(3). As can be seen from Table 2, the overall  $k$  is 0.81 for all tests. A Cohen–Kappa coefficient of 0.81 or above is indicative of a “strong” or “almost perfect agreement” between the two methods.<sup>34</sup> Since the Cohen–Kappa coefficient only defines how consistent the results are amongst the tests being compared, additional analysis was performed to predict the accuracy of the PEF and qPCR leaf tests compared to the Las status of the trees from which the leaves were harvested.

**III.3.2 Comparison through predictions against the Las status of the tree.** The second comparison aimed to define the sensitivities and specificities of the tests performed on the individual leaves using either the PEF or qPCR against the known Las status of the trees from which the leaves were harvested. Using the above defined cutoff values, the obtained sensitivity and specificity by PEF and qPCR for GFT, PUM, LEM, and VAL, and the average sensitivity and specificity for all leaves were determined and listed in Table 1. As can be seen, qPCR exhibited an overall 100% specificity *versus* PEF's overall 90% specificity, indicating qPCR is more specific than the PEF elastic modulus measurements, *i.e.*, qPCR had fewer false positives than PEF. On the sensitivity side, PEF exhibited an overall 94% sensitivity as compared to qPCR's 89% sensitivity, suggesting PEF is more sensitive than qPCR in predicting the Las status of the trees from which the leaves were harvested and could yield fewer false negative tests.

To show where PEF's elastic modulus measurements were more sensitive than qPCR, we plotted the Ct values obtained by qPCR *versus* the PEF elastic moduli measured in GFT, PUM, LEM, and VAL leaves in Fig. 5(a)–(d), respectively. The vertical dashed lines indicate the cutoff elastic modulus (611, 598, 575, and 602 kPa for GFT, PUM, LEM, and VAL, respectively) while the horizontal dashed lines indicate the cutoff Ct values for qPCR (Ct = 36 for all leaves). In each figure, the upper left quadrant is where PEF results are negative, and qPCR results are positive ( $N_{\text{PEF}}, P_{\text{qPCR}}$ ). The upper right quadrant is where both PEF and qPCR results are positive ( $P_{\text{PEF}}, P_{\text{qPCR}}$ ). The lower left quadrant is where both PEF and qPCR results are negative



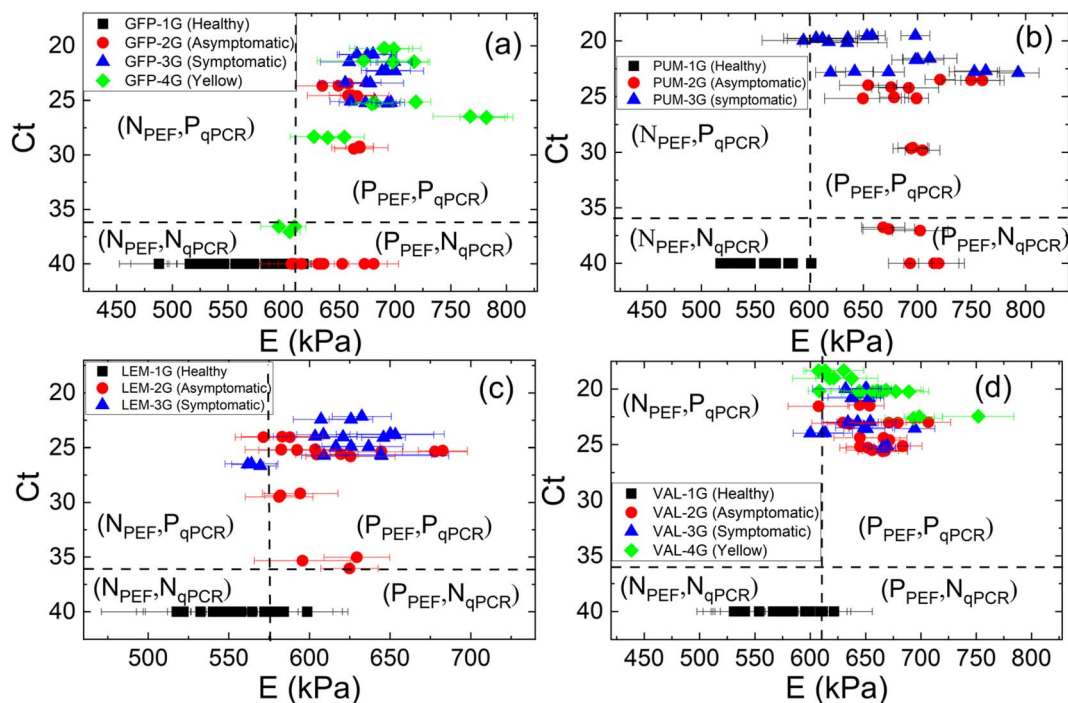


**Fig. 5** Ct values from qPCR versus the elastic modulus ( $E$ ) as measured by PEF of (a) GFT, (b) PUM, (c) LEM, and (d) VAL. The vertical dashed lines indicate the cutoff elastic modulus (611, 598, 575, and 602 kPa for GFT, PUM, LEM, and VAL, respectively) while the horizontal dashed lines indicate the cutoff Ct for qPCR ( $Ct = 36$  for all leaves). Each figure has four quadrants. The upper left ( $N_{PEF}, P_{qPCR}$ ) quadrant is where PEF results are negative, and qPCR results are positive. The upper right ( $P_{PEF}, P_{qPCR}$ ) quadrant is where both PEF and qPCR results are positive. The lower left ( $N_{PEF}, N_{qPCR}$ ) quadrant is where both PEF and qPCR results are negative. The lower right ( $P_{PEF}, N_{qPCR}$ ) quadrant is where PEF results are positive, and qPCR results are negative. Most of the diseased leaves (circles, triangles, and diamonds) fall in the ( $P_{PEF}, P_{qPCR}$ ) quadrant and most of the healthy leaves (squares) fall in the ( $N_{PEF}, N_{qPCR}$ ) quadrant, indicating agreement between the two methods. Further comparison indicates qPCR as more specific than PEF – *i.e.*, PEF had false positives while qPCR had none (see black squares in the lower right quadrant). However, PEF is more sensitive than qPCR, particularly for asymptomatic leaves as can be seen in (a) and (b) which show that qPCR missed substantially more asymptomatic GFT and PUM leaves (circles) than PEF.

( $N_{PEF}, N_{qPCR}$ ). The lower right ( $P_{PEF}, N_{qPCR}$ ) quadrant is where PEF results are positive, and qPCR results are negative. From Fig. 5(a)–(d), one can see that most leaves from  $Las^+$  trees (circles, triangles, and diamonds) fall in the upper right quadrant ( $P_{PEF}, P_{qPCR}$ ), consistent with a “strong” or “almost perfect” agreement between the predictions of the two methods as indicated by a Cohen–Kappa coefficient of 0.81. A closer look at Fig. 5(a) and (b) shows that many asymptomatic GFT and PUM leaves were missed by qPCR but not PEF, indicating PEF is more sensitive in detecting HLB in asymptomatic leaves than qPCR. In Table 3 we summarize the sensitivities of PEF and qPCR for

asymptomatic leaves of GFT, PUM, LEM, and VAL. Clearly, the sensitivities of PEF were higher than qPCR with the average sensitivity of PEF being 96% for all symptomatic leaves while the average sensitivity of qPCR was only 78% for all the same asymptomatic leaves. Meanwhile, Fig. 5(a) seems to suggest that both qPCR and PEF had more false negatives for yellowing leaves than other  $Las^+$  positive leaves. This could be due to the degradation of yellowing leaves, leading to the decrease in leaf elastic modulus and in the amount of *Las* bacterial DNA. Therefore, it will be of interest to examine the results of PEF and PCR tests of yellowing leaves longitudinally with time to find out at what time point the elastic modulus and *Las* titer decrease so much as to become indistinguishable from those of  $Las^-$  leaves.

**Table 3** Comparison of asymptomatic HLB detection of PEF with qPCR of the same leaves

Asymptomatic		Sensitivity	
Citrus	$n$	PEF	qPCR
Grapefruit	18	89%	50%
Pumelo	18	100%	67%
Lemon	18	94%	94%
Valencia	18	100%	100%
<b>All</b>	<b>72</b>	<b>96%</b>	<b>78%</b>

## IV. Discussions

Elasticity has been used to measure tolerances to abiotic stress such as drought when comparing leaf tissues across entirely different species.<sup>35</sup> However, it has not been used for pathogen identification. Results from four major citrus species/hybrids demonstrated a direct correlation between the elastic modulus and the presence of *Las*. Furthermore, low-titer, asymptomatic leaves were delineated from healthy (non-



infected) leaves even more sensitively with PEF than qPCR, which is critical for early-stage detection and demonstrates the utility of mechanical measurements as an early screening method for HLB. Given that the measurements obtained are also quantitative, data may be assessed and tracked using predictive mathematical modelling. Use of the PEF as a screening platform for HLB has many advantages over the current industry standard of qPCR-based methods. For example, the PEF does not require expensive equipment to operate nor are consumables required for testing. In addition, the simplicity of the PEF eliminates the need for highly trained personnel to perform the testing and expands testing capabilities to citrus producers and/or field workers, which will reduce testing costs on a per sample basis. Because this technology also allows testing to be performed in the field and yields results instantaneously, it decreases the turnaround time for results, which is one of the most important factors for preventing spread. Even if used only as a screening device, the PEF will help save resources by eliminating the large number of negative samples that are undergoing the tedious qPCR testing process. Because the device utilizes a non-destructive sampling method, it may also prove useful for identifying new cultivars that are either resistant or show tolerance to HLB, which are a critical component to reviving the citrus industry in areas where HLB is endemic such as the Southeastern portion of the United States. Additionally, it would allow new therapeutics to be evaluated at a much earlier stage than present detection methods allow, which results in both time and cost-savings.

Our use of fully expanded mature leaves 6–10 cm long was important for several reasons. For one, many features of mature tissue, including the symplasmic water content, leaf volume per unit leaf area, diameter of a palisade tissue cell, cell wall thickness and the bulk elastic modulus are relatively stable at this point in development since they have passed the transitioned point from sink to source.<sup>36</sup> In addition, surface characteristics of citrus leaves such as the cuticle components and thickness also remain consistent by this time.<sup>37</sup> Selection of mature tissue is beneficial from the aspect of timing as well since citrus does not drop its leaves on an annual basis,<sup>38</sup> therefore mature leaves should be present anytime testing is desired. To illustrate this point, we show in Fig. 6(a) and (b) respectively the elastic moduli of healthy 1 year-old GFT leaves (open squares) and that of healthy 3 year-old GFT leaves (full squares), and the elastic modulus distribution of healthy 1 year-old GFT leaves (square-shaded bars and dash-dotted line) and that of healthy 3 year-old GFT leaves (line-shaded bars and dash-dot-dotted line) obtained with a polydimethylsiloxane (PDMS) leaf sample holder with an elastic modulus of 330 kPa. As can be seen, the elastic moduli of the healthy 1 year-old and healthy 3 year-old GFT leaves were indistinguishable. This is in direct contrast to immature leaves, which may or may not be present given that flushing of trees occurs on a seasonal or annual basis in citrus.

The elastic moduli of the healthy leaves can differ depending upon the citrus species, age, field location, management condition, climate, altitude, season, and other factors. However, such factors can be quantified using PEF to establish a citrus

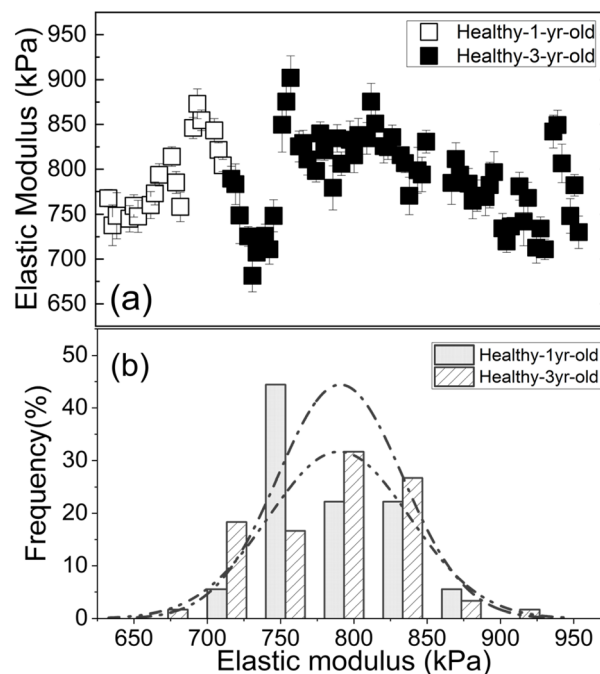


Fig. 6 (a) The elastic moduli of healthy 1 year-old GFT leaves (open squares) and that of healthy 3 year-old GFT leaves (full squares), and (b) the elastic modulus distribution of healthy 1 year-old GFT leaves (square-shaded bars and dash-dotted line) and that of healthy 3 year-old GFT leaves (line-shaded bars and dash-dot-dotted line).

leaf elasticity baseline to permit proper control for the citrus species, field location, management condition, altitude, climate, season, management conditions, and other factors. For example, the elastic moduli for the healthy 1 year-old and 3 year-old GFT leaves shown in Fig. 6(a) were higher and those of the healthy GFT leaves shown in Fig. 4(a). One reason was that elastic moduli in Fig. 6(a) were obtained with a PDMS leaf sample holder with an elastic modulus of 330 kPa whereas those in Fig. 4(a) were obtained with a gelatin leaf sample holder with an elastic modulus of 210 kPa. The higher elastic modulus of the PDMS leaf sample holder increased the leaf elastic moduli values in Fig. 6(a). Furthermore, the leaves in Fig. 6(a) were harvested in January whereas those for Fig. 4(a) were harvested in August, which may also affect the measured elastic moduli. However, our view is that so long as we have proper control of healthy citrus samples, we will be able to overcome the influence from these variable factors. Taken together, utilization of the PEF as a screening device for HLB will allow more samples to be tested by HLB surveillance programs. Based on the low-cost and portability of its breast cancer detector predecessor, we believe the PEF elasticity detector can be developed into an automated field-usable tool for HLB screening that users do not need to assemble.

Since PEF rely on increased leaf elastic modulus to screen for HLB, one question may arise as to whether PEF leaf elasticity measurement could differentiate HLB-positive leaves from other diseased leaves such as Citrus Tristeza Virus (CTV)-positive leaves that are also known to be stiffer than healthy leaves.<sup>39</sup> Our view is that leaf elasticity alone may not be



sufficient to differentiate between different infections just like not all stiffer breast lesions are breast cancers but it can be a useful *screening* tool to identify diseased plants for *early qPCR diagnosis*, which is important for plant protection. Without screening, early HLB detection by qPCR alone has proven ineffective much like detecting breast cancer before mammography *screening* when breast cancers were usually found late with a much higher mortality rate.<sup>40,41</sup> To improve delineation of HLB from other infections other changes associated with HLB such as leaf thickness changes and leaf color pattern changes may also quantify together with leaf elasticity changes to provide a more comprehensive comparison, which is warranted in a future study. Finally, as we have shown that a PEF with a 0.4 mm probe is more sensitive than a PEF with a 0.6 mm probe; it is conceivable that a PEF with a probe smaller than 0.4 mm in diameter may be even more sensitive for detecting HLB. This, along with additional comparisons with qPCR, will be explored in a separate future publication.

## V. Conclusion

We have evaluated using a piezoelectric finger (PEF) with a 0.4 mm probe to measure the elastic modulus of a leaf to detect the presence of Las in four major citrus species/hybrids including grapefruit (GFT), pumelo (PUM), lemon (LEM), and Valencia orange (VAL). Leaves were harvested from Las positive trees and included both symptomatic (*i.e.*, blotchy mottle or yellowing) as well as asymptomatic leaves (those without visual symptoms). The healthy leaves were harvested from trees that tested negative for Las. The results indicated that the PEF elastic modulus test exhibited an overall 94% sensitivity and 90% specificity against the Las status of the trees for all four types of citrus trees combined. Comparison qPCR tests on the same leaves showed an overall 89% sensitivity and 100% specificity against the Las status of the trees. While a Cohen–Kappa coefficient of 0.81 was obtained between the PEF and qPCR predictions, suggesting a “strong” agreement between the PEF and qPCR tests, more detailed examination indicated that PEF was more sensitive overall in detecting the Las positive trees than qPCR, particularly from asymptomatic leaves, indicating the potential of using PEF for early detecting HLB.

## Data availability

Data will be available upon request.

## Conflicts of interest

WY Shih and WH Shih founded Intelligent Sentinel LLC to commercialize the PEF HLB detector. All the other authors have no conflicts of interest.

## Acknowledgements

The authors would like to acknowledge the support by the United States Department of Agriculture (USDA) under ARSX Trust Fund Cooperative Agreement no. 58-8072-0-017. Mention

of trade names or commercial products in this publication is solely for the purpose of providing specific information and does not imply recommendation or endorsement by the USDA. The USDA is an equal opportunity employer.

## Notes and references

- 1 C. Zhou, *Trop. Plant Pathol.*, 2020, **45**, 6.
- 2 J. M. Bove, *J. Plant Pathol.*, 2006, **88**, 31.
- 3 D. Ghosh, S. Kokane, B. K. Savita, P. Kumar, A. K. Sharma, A. Ozcan, A. Kokane and S. Santra, *Plants*, 2023, **12**, 160.
- 4 D. Thakuria, C. Chaliha, P. Dutta, S. Sinha, P. Uzir, S. B. Singh, S. Hazarika, L. Sahoo, L. L. Kharbikar and D. Singh, *Physiol. Mol. Plant Pathol.*, 2023, **125**, 102016.
- 5 F. Ding, S. A. Peng and J. S. Hartung, *Plant Dis.*, 2020, **104**, 1584–1588.
- 6 E. Baldwin, A. Plotto, J. Manthey, G. McCollum, J. Bai, M. Irey, R. Cameron and G. Luzio, *J. Agric. Food Chem.*, 2010, **58**, 1247–1262.
- 7 T. R. Gottwald, *Annu. Rev. Phytopathol.*, 2010, **48**, 119–139.
- 8 L. J. Zhou, D. W. Gabriel, Y. P. Duan, S. E. Halbert and W. N. Dixon, *Plant Dis.*, 2007, **91**, 227.
- 9 P. A. Stansly, H. A. Arevalo, J. A. Qureshi, M. M. Jones, K. Hendricks, P. D. Roberts and F. M. Roka, *Pest Manage. Sci.*, 2014, **70**, 415–426.
- 10 J. A. Tansey, P. Vanaclocha, C. Monzo, M. Jones and P. A. Stansly, *Pest Manage. Sci.*, 2017, **73**, 904–916.
- 11 Z. Yan, J. Rascoe, L. B. Kumagai, M. L. Keremane and M. K. Nakhla, *Plant Dis.*, 2016, **100**, 645.
- 12 Animal and Plant Health Inspection Service, *Asian Citrus Psyllid*, 2022, <https://www.aphis.usda.gov/aphis/ourfocus/planthealth/plant-pest-and-disease-programs/pests-and-diseases/citrus/acp>, accessed May 19, 2022.
- 13 J. A. Lee, S. E. Halbert, W. O. Dawson, C. J. Robertson, J. E. Keesling and B. H. Singer, *Proc. Natl. Acad. Sci. U. S. A.*, 2015, **112**, 7605–7610.
- 14 M. L. Keremane, T. G. McCollum, M. L. Roose, R. F. Lee and C. Ramadugu, *Plants*, 2021, **10**, 2111.
- 15 W. B. Li, L. Levy and J. S. Hartung, *Phytopathology*, 2009, **99**, 139–144.
- 16 A. Pourreza, W. Suk Lee, E. Raveh, Y. Hong and H.-J. Kim, *Presented in Part at the 2013 Kansas City, Missouri, July 21 - July 24, 2013, St. Joseph, MI*, 2013.
- 17 T. Gottwald, G. Poole, T. McCollum, D. Hall, J. Hartung, J. Bai, W. Luo, D. Posny, Y. P. Duan, E. Taylor, J. da Graca, M. Polek, F. Louws and W. Schneider, *Proc. Natl. Acad. Sci. U. S. A.*, 2020, **117**, 3492–3501.
- 18 M. S. Hassan and R. Lau, *Int. J. Pharm.*, 2010, **386**, 6–14.
- 19 D. S. Achor, E. Etxeberria, N. Wang, S. Y. Folimonova, K. R. Chung and L. G. Albrigo, *Plant Pathol. J.*, 2010, **9**, 56–64.
- 20 L. G. Albrigo and E. W. Stover, *Horttechnology*, 2015, **25**, 785–790.
- 21 S. Y. Folimonova and D. S. Achor, *Phytopathology*, 2010, **100**, 949–958.
- 22 E. J. Koh, L. J. Zhou, D. S. Williams, J. Park, N. Y. Ding, Y. P. Duan and B. H. Kang, *Protoplasma*, 2012, **249**, 687–697.



- 23 X. Xu, C. Gifford-Hollingsworth, R. Sensenig, W. H. Shih, W. Y. Shih and A. D. Brooks, *J. Am. Coll. Surg.*, 2013, 1168.
- 24 X. Xu, Y. Chung, A. D. Brooks, W. H. Shih and W. Y. Shih, *Rev. Sci. Instrum.*, 2016, **87**, 124301.
- 25 A. Markidou, W. Y. Shih and W. H. Shih, *Rev. Sci. Instrum.*, 2005, **76**, 064302.
- 26 S. T. Szewczyk, W. Y. Shih and W. H. Shih, *Rev. Sci. Instrum.*, 2006, **77**, 044302.
- 27 X. Xu, W. H. Shih and W. Y. Shih, *Rev. Sci. Instrum.*, 2019, **90**, 015006.
- 28 H. Yegingil, W. Y. Shih and W. H. Shih, *Rev. Sci. Instrum.*, 2007, **78**, 115101.
- 29 H. Yegingil, W. Y. Shih and W. H. Shih, *Rev. Sci. Instrum.*, 2010, **81**, 095104.
- 30 M. M. Doud, Y. S. Wang, M. T. Hoffman, C. L. Latza, W. Q. Luo, C. M. Armstrong, T. R. Gottwald, L. Y. Dai, F. Luo and Y. P. Duan, *Hortic. Res.*, 2017, **4**, 17054.
- 31 L. J. Zhou, C. A. Powell, M. T. Hoffman, W. B. Li, G. C. Fan, B. Liu, H. Lin and Y. P. Duan, *Appl. Environ. Microbiol.*, 2011, **77**, 6663–6673.
- 32 W. W. Turechek, M. Irely, P. Sieburth, R. Brlansky, J. DaGraça, J. Graham, T. Gottwald, J. Hartung, M. Hilf, M. Kunta, K. Manjunath, H. Ling, C. Ramdugu, P. Roberts, M. Rogers, R. Shatters, X. Sun and N. Wang, *Presented in Part at the Proceedings of International Research Conference on Huanglongbing*, Orlando, Florida, 2009.
- 33 M. Irely, P. Sieburth, R. Brlansky, J. DaGraça, J. Graham, T. Gottwald, J. Hartung, M. Hilf, M. Kunta, K. Manjunath, H. Ling, C. Ramdugu, P. Roberts, M. Rogers, R. Shatters, X. Sun and N. Wang, *Presented in Part at the Proceedings of International Research Conference on Huanglongbing*, Orlando, Florida, 2008.
- 34 M. L. McHugh, *Biochem. Med.*, 2012, **22**, 276–282.
- 35 D. Xing, X. Chen, Y. Wu, Q. Chen, L. Li, W. Fu and Y. Shu, *J. Plant Interact.*, 2019, **14**, 7.
- 36 Y. Tazoe, K. Noguchi and I. Terashima, *Plant, Cell Environ.*, 2006, **29**, 691–700.
- 37 E. A. Baker, J. Procopiu and G. M. Hunt, *J. Sci. Food Agric.*, 1975, **26**, 9.
- 38 C. Ribeiro, J. Xu, D. Teper, D. Lee and N. Wang, *Plant Mol. Biol.*, 2021, **106**, 349–366.
- 39 S. Fu, J. Shao, C. Zhou and J. S. Hartung, *Front. Plant Sci.*, 2017, **8**, 1419.
- 40 H. Weedon-Fekjaer, P. R. Romundstad and L. J. Vatten, *Br. Med. J.*, 2014, **348**, g3701.
- 41 S. W. Fletcher and J. G. Elmore, *N. Engl. J. Med.*, 2003, **348**, 1672–1680.

